PACS: 62.20.Fe

Y. Beygelzimer[1], V. Varyukhin[1], R. Kulagin[2], D. Orlov[3]

TWIST EXTRUSION: REVIEW

[1]Donetsk Institute for Physics and Engineering named after A.A. Galkin, National Academy of Sciences of Ukraine

[2]Institute of Nanotechnology, Karlsruhe Institute of Technology (KIT), Germany

[3]Lund University, Division of Materials Engineering, Sweden

Received October 26, 2015

The review of research on the twist extrusion (TE) made in Donetsk Institute for Physics and Engineering of National Academy of Sciences of Ukraine since 1999 is reported. The main features of twist extrusion are presented. It is noted Twist Extrusion has a significant commercial potential due to the following physical effects: intensive grain refinement; homogenization and mixing; intensive consolidation of powders. The engineering relations for the major Twist Extrusion characteristics are obtained. The progress in practical application of this process is shown.

Keywords: twist extrusion, severe plastic deformation, simple shear, grain refinement

Представлено огляд досліджень з гвинтової екструзії (ГЕ), виконаних у ДонФТІ починаючи з 1999 р. Показано, що ГЕ має значний комерційний потенціал у зв'язку з наступними фізичними ефектами: інтенсивним подрібненням структури матеріалів; гомогенізацією і перемішуванням на різних масштабних рівнях; інтенсивною консолідацією порошкових матеріалів. Наведено інженерні співвідношення для основних характеристик ГЕ. Показано прогрес у практичному застосуванні ГЕ.

Ключові слова: гвинтова екструзія, інтенсивна пластична деформація, субмікрокристалічні матеріали, простий зсув, подрібнення зерен

Introduction

Twist extrusion (TE) is a severe plastic deformation technique. It was proposed in 1999 in Donetsk Institute for Physics and Engineering of National Academy of Sciences of Ukraine [1]. In this anniversary year for the Institute, TE has reached the age of majority. This is the beginning of adult life and the onset of full legal capacity. The purpose of this review is to show how the TE is prepared for this life. Many laboratories in the world perform research with using TE now. This review presents mainly the achievements reached at Donetsk Institute for Physics and Engineering.

1. Historical retrospective

TE is a technique where a billet is extruded through a constant cross-section die having two prismatic sections separated by a helical one in between. This allows the accumulation of plastic strain in the billet without the alteration of its net shape. Such a property makes possible the accumulation of very large (or severe) strains when multiple pass extrusion is employed. The principal scheme of a channel in the die for twist extrusion is shown in Fig. 1 along with a billet before and after a passage through the TE die.

The profile of a TE die cross-section can be arbitrary. A few examples of possible profiles are shown in Fig. 2.

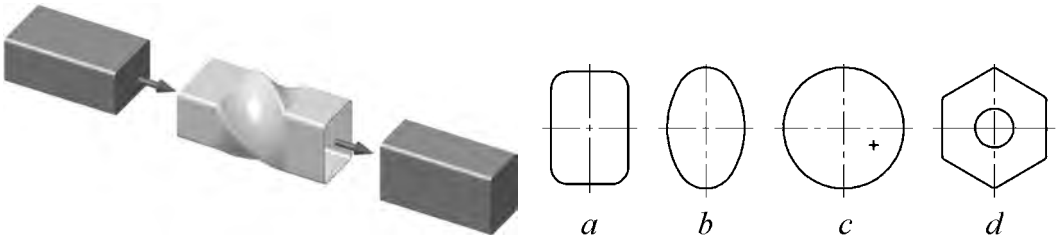

Fig. 1. Scheme illustrating twist extrusion

Fig. 2. A few examples of cross-sections of dies for twist extrusion: *a* – rectangular; *b* – elliptical; *c* – circular, '+' denotes the position of extrusion axis; *d* – hexagonal with a hollow centre

Let us emphasise here a principal ability of TE to process bars having circular cross-section profile. This can be achieved when the axis of extrusion is shifted away from the axis of symmetry of the channel. It is illustrated in Fig. 2,*c* where the extrusion axis indicated by '+' is located aside from the centre of symmetry of the channel in the middle of the cross-section. Tubular billets with a hollow centre can also be processed by TE when extrusion on a barrel is used, Fig. 2,*d*.

Due to the wide experience of work with hydro extrusion in the Donetsk Institute for Physics and Engineering, the first tool set implementing the idea of TE was based on a hydro extrusion machine. A pre-existing tool set for hydro extrusion was converted into the tool set for hydro mechanical twist extrusion as illustrated in Fig. 3. A brief description of this tool set work is as follows. A billet *3* with the rectangular cross-section of 14 × 16 mm and the length of 60 mm is extruded through TE die *4*. The die sits on a supporting liner *5*, which stays on a conical die *7*. This conical die is used for the direct extrusion of a dummy billet. The channel of high-pressure container *2* is filled with a working fluid, a mineral oil I-20. After that, punch *1* compresses the working fluid thus increasing a hydrostatic pressure in the container. At the pressure of 600–700 MPa, the dummy billet begins to extrude through the conical die *7*, while the punch moving along the container axis pushes billet *3* through TE die *4*. When the punch touches the top edge of TE die, the process is stopped. Then, a new dummy billet is installed to the conical die, the TE die is flipped for 180°, and the process is repeated.

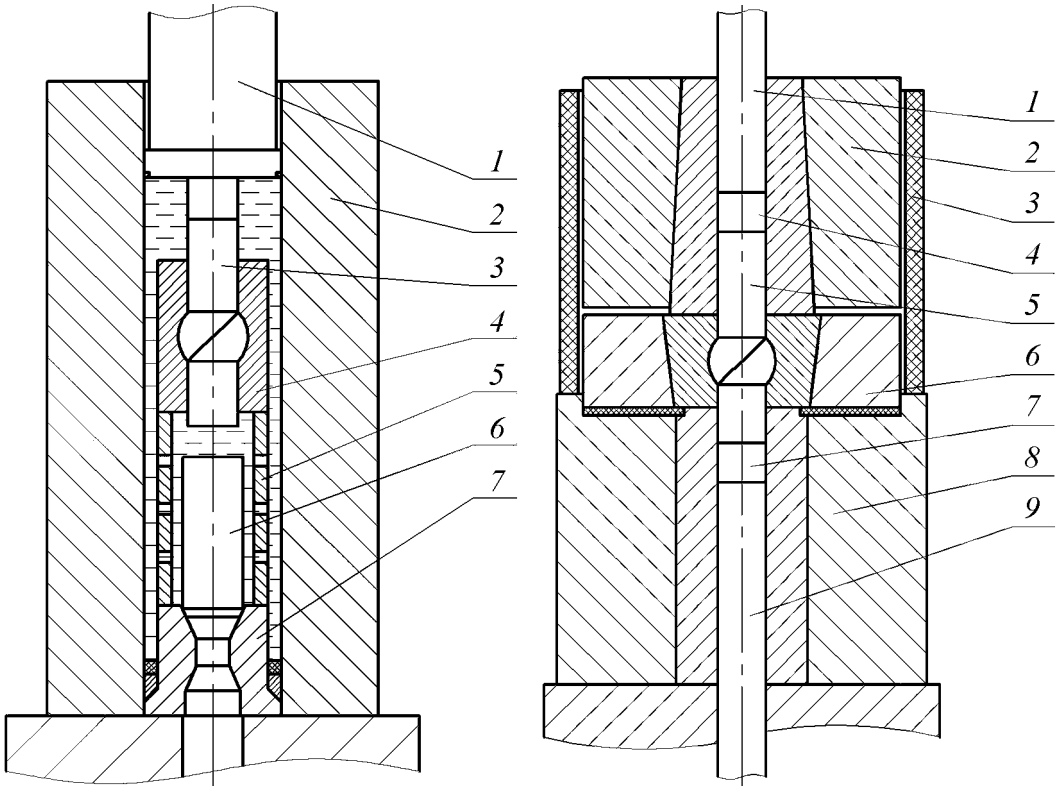

Fig. 3. Scheme of the first tool set for the hydromechanical twist extrusion

Fig. 4. Scheme of the first tool set for the mechanical twist extrusion

The main advantage of hydro mechanical TE is that the process is carried out under high hydrostatic pressure without friction of the billet on the channel walls. The main disadvantage of this scheme is very low productivity of the process. Therefore, this tool set was re-designed, and a new tool set for a mechanical TE more similar to a conventional direct extrusion was adopted in the department. The first tool set is illustrated in Fig. 4. It is composed by two-layered upper container *2* and a two-layered TE die *6* of the same cross-section. The die has the slope of twist line to extrusion axis 30–60°. The outlet cross-section is twisted with regard to the inlet by the angle of 30–120°. The bottom part of TE die has a minor decrease of the channel cross-section to compensate for residual elastic stresses and other distortion defects in the billet being processed. Receiving container *8* having the same cross-section is located underneath the die. It also serves to prevent plastic deformation of the billet outside the die when a back-pressure is used. The upper container and the die are encased into a resistance heater *3*, which allows the processing at the temperatures elevated up to 450°C.

A typical extrusion cycle is as follows. A plunger for back pressure *9* is inserted through the bottom container *8* up to the exit from the helical part of TE die *6*. A dummy billet is pressed into the helical part of the die. A billet to be processed *5* and another dummy billet *4* are loaded into the upper container *2*. Then, all the billets are extruded through the die by a main plunger *1*. During the extru-

sion, the back pressure is maintained at a level of 0.5–1.0 σ_s (where σ_s is the flow stress of the billet material) to ensure appropriate kinematics of plastic flow. In addition, this level of back pressure minimises the loss of ductility of a material being processed due to a high hydrostatic pressure in the centre of deformation [2], so that even hard to deform materials can be processed. The extra dummy billet *4* is needed to extrude the entire main billet through TE die 'in one pass'. After the extrusion cycle, the main billet *5* and the dummy billet *7* come out from the bottom container, while the dummy billet *4* remains in the helical part of the die. At this stage, the extrusion cycle can be repeated, if required.

As the dummy billets, copper (Cu), zinc (Zn) and their alloys were used. The lubricants used to be selected based on a material to be processed and processing regimes. For the extrusion at ambient temperatures, Teflon, beeswax, rosin, and castor oil were used. For the extrusion at elevated temperatures, low melting point glassy lubricants based on lead (Pb) and Zn oxides were utilised.

The results of the experiments performed utilising the aforementioned tool sets as well as the first theoretical studies of TE have been rather well reported in [3–5]. The effectiveness of TE processing for microstructure and property tailoring in metallic materials have been proven for titanium (Ti) alloys Cp Ti Grades 2 and 6, VT-22, VT3-1; Super alloy Inconel 718; Al-Mg-Sc alloys; recycled grades of copper-phosphorus and aluminium alloys AK9, AM5M2, AV87, etc.

At the moment, three directions of applications of TE processing can be highlighted:

– manufacturing of bulk nanostructured materials through grain refinement, cf. [3–23];

– improvement of ductility in recycled non-ferrous alloys, cf. [24];

– manufacturing of bulk nanostructured materials through powders consolidation, cf. [25].

In every direction, collaboration with industrial partners had been established. Namely, in collaboration with 'Motor Sich', technologies for turbine blades manufacturing from nanostructured Ti alloys and chemically homogeneous Ti alloy wires for mono wheels restoration are being developed. In collaboration with 'Zaporozhskiy titano-magieviy kombinat', a technology for Ti sponge consolidation into electrodes for electro slag refining, have been developed. In collaboration with JSC 'Donsplav', a technology for chemical homogeneity improvement in recycled non-ferrous alloys has been designed. In collaboration with GE Global Research, Ti-6-4 and Inconel 718 were processed by TE. In collaboration with Boeing, properties in Al alloys for aviation were tailored by TE processing.

Now, a pilot industrial tool set for TE processing has been established in Donetsk Institute for Physics and Engineering on the National Academy of Sciences – Ukraine. It allows the processing of billets with dimensions of 30 × 40 × 140 mm at the amount of 1200 kg per year. This pilot industrial line is designed to manufacture nanostructured titanium.

2. Mechanics of plastic flow in twist extrusion

In this subsection, characteristic features of TE are considered and compared to equal channel angular extrusion (ECAE) and high pressure torsion (HPT). Then, the results of experimental and theoretical investigations of stress-strain state in TE processing are presented. In particular, the minimal level of back pressure to ensure the kinematics of plastic flow in TE is determined; a vortex-like plastic flow within TE channel cross-section is revealed; and the effect of strain hardening on plastic flow in TE is investigated.

2.1. Characteristic properties of deformation in twist extrusion

As has been revealed by comprehensive experimental and theoretical investigations over the last decade [3,6,14,16,18,22,26,27], major features of plastic flow during TE were grasped with a simplistic kinematically admissible velocity field proposed already in early work [28]:

$$V_x = -\frac{yV_0 \tan\beta}{R}, \quad V_y = \frac{xV_0 \tan\beta}{R}, \quad V_z = -V_0 , \tag{1}$$

where x, y, z are coordinates, axis z coincides with TE die axis of symmetry, V_0 is the velocity of a billet move along z axis, R is the radius of circumference on the channel cross-section periphery, β is the angle of twist line slope on the channel cross-section periphery.

The field of velocities (1) presumes that each virtual cross-sectional layer of the billet acts as a solid having translational displacements along the extrusion axis and a rotational one about the axis. No distortion of the layer in z direction is possible. This field of velocities is reduced to the following tensor of strain rates:

$$\begin{gathered} \dot{e}_{xx} = \dot{e}_{yy} = \dot{e}_{zz} = \dot{e}_{xy} = 0, \\ \dot{e}_{xz} = -\frac{yV_0}{2R\cos^2\beta}\frac{\mathrm{d}\beta}{\mathrm{d}z}, \\ \dot{e}_{yz} = \frac{xV_0}{2R\cos^2\beta}\frac{\mathrm{d}\beta}{\mathrm{d}z}. \end{gathered} \tag{2}$$

Substituting (2) in the expression for the intensity of strain rates:

$$\dot{e}_i = \frac{\sqrt{2}}{3}\sqrt{\left(\dot{e}_{xx}-\dot{e}_{yy}\right)^2 + \left(\dot{e}_{xx}-\dot{e}_{zz}\right)^2 + \left(\dot{e}_{yy}-\dot{e}_{zz}\right)^2 + 6\left(\dot{e}^2{}_{xy} + \dot{e}^2{}_{xz} + \dot{e}^2{}_{yz}\right)}, \tag{3}$$

we obtain a relation for the calculation of the strain rate intensity at any point of the deformation zone:

$$\dot{e}_i = \frac{1}{\sqrt{3}}\frac{rV_0}{R\cos^2\beta}\left|\frac{\mathrm{d}\beta}{\mathrm{d}z}\right|. \tag{4}$$

Integrating equation (4) by time from the moment of a material point entrance to TE die until its exit from there, we obtain an estimate for Von Mises equivalent strain:

$$e_i = \frac{2}{\sqrt{3}} \frac{r}{R} \tan\beta . \qquad (5)$$

Equation (4) suggests that the majority of strain accumulates sharply in thin zones of simple shear deformation located in the vicinities of entrance and exit from the helical part of TE die where $\left|\frac{d\beta}{dz}\right|$ has extreme values. Since derivatives of β in these zones have opposite signs, deformation in TE processing is principally reversal.

The simple form of equation (5) suggests that the accumulated strain decreases linearly from a billet periphery towards axis where it is equal to zero. However, later results, both experimental and theoretical, revealed that although accumulated net strain after TE processing is heterogeneous indeed, the strain at a billet axis is well above nil. These results have been partially reported elsewhere [3,6,8,11,16,18,26,27,29], and are comprehensively presented in the following subsection.

Now, let's compare TE with other two popular severe plastic deformation (SPD) techniques, high pressure torsion (HPT) and equal channel angular extrusion (ECAE). In all these processes, net shape of a billet does not change substantially during processing, and a dominating deformation mode is simple shear. However, in spite of ECAE where the shear direction is inclined at 45° to the extrusion axis, in TE the shear direction is perpendicular to it. In the later process, net strain is heterogeneous within the billet cross-section similar to HPT. Comparing equations (5) and $e_{\text{tor}} = \frac{r\varphi}{\sqrt{3}h}$ (where r and h are HPT sample radius and thickness, respectively; φ is the torsion angle), typically used for the calculation of Von Mises strain in HPT, one can see that each zone of most intense simple shear in TE can be envisaged as a pair of HPT dies having specific torsion angle $\frac{\varphi}{h} = \frac{\tan\beta}{R}$. Therefore, TE can also be imagined as an extrusion through two pairs of 'transparent' HPT anvils, to a certain extent, as illustrated in Fig. 5.

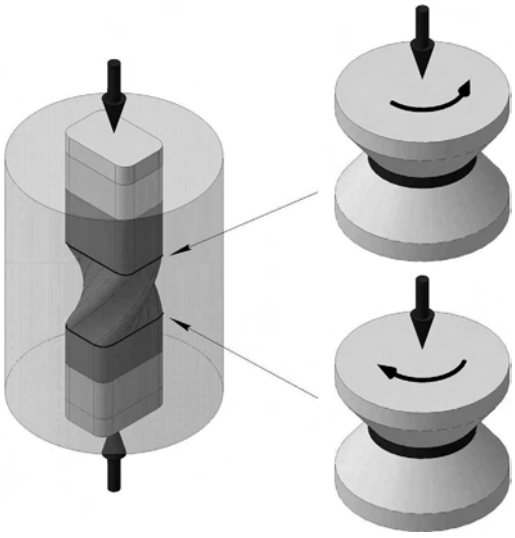

Fig. 5. Analogy of TE and two pairs of HPT dies

The dies for twist extrusion may have two different directions of twist: a clockwise die (CD) and a counterclockwise die (CCD). A sequential transition from CD to CCD or vice versa allows flipping the direction of shear between passes therefore leading to two main routes of TE:

– route I – CD + CD (or CCD + + CCD);

– route II – CD + CCD (or CCD + CD).

It is obvious that if route I imparts strain with amplitude $\Delta e_i^{\mathrm{I}} = \frac{1}{\sqrt{3}}\frac{r}{R}\tan\beta$, in route II the amplitude is $\Delta e_i^{\mathrm{II}} = 2\frac{1}{\sqrt{3}}\frac{r}{R}\tan\beta$.

The last but not the least peculiarity of twist extrusion we would like to discuss in this subsection is the increase of billet surface in the helical part of TE die. Depending on specific die design, the area of lateral surface of a billet being processed increases for 30–50% upon entering the helical part of TE die, and then returns to the initial surface area upon exit. After multi-pass processing, such an effect leads to significant stirring of inner and outer layers of a billet being processed. This can be utilised as an extra option for the modification of structure and properties if TE is carried out using surfactant fluids as lubricants [18].

2.2. Stress-strain state in twist extrusion

The stress-strain state during twist extrusion for different dies, processing conditions and materials have been studied both theoretically, e.g. [3,6,26,29–32], and experimentally, e.g. [3,6,14,27,30,33]. Compared to the ideas presented above, these studies significantly advanced understanding of plastic flow and capabilities of twit extrusion.

At the first place, they revealed that to ensure the kinematics of plastic flow and complete filling of channel in TE die during processing, a back pressure of at least half the flow stress of a material being processed should be applied [3,6,29,32]. The exact value of the back pressure depends on the profile of the TE channel cross-section, the rate of strain hardening, and friction. To illustrate the effect of incomplete filling of the die channel, photographs of Cp Ti billets after TE processing with different levels of back pressure are presented in Fig. 6 along with corresponding schematics.

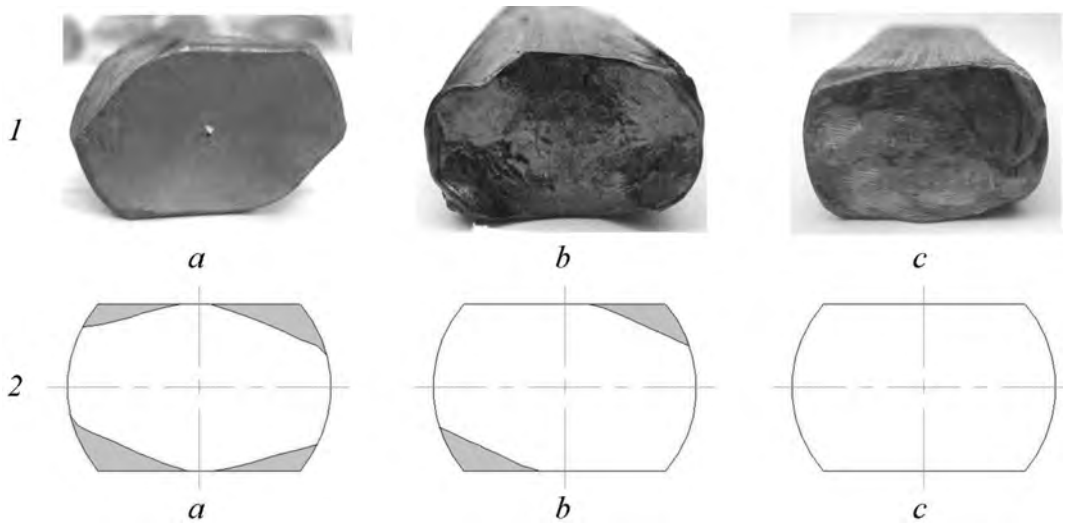

Fig. 6. Photographs of Cp Ti billets (*1*) and corresponding schematics of filling of TE die channel (*2*) after processing at different levels of back pressure: *a* – no back pressure, *b* – back pressure ~ $0.5\sigma_s$, *c* – back pressure ~ $1.0\sigma_s$; σ_s is flow stress

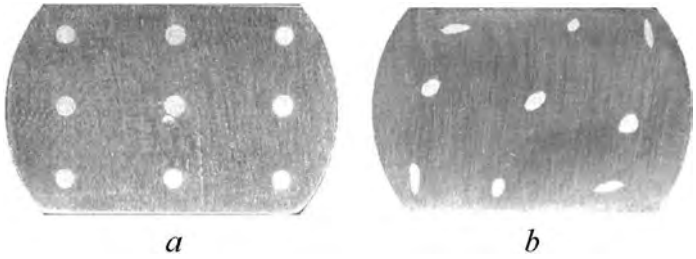

Fig. 7. Cross-sectional view of a copper billet with embedded aluminium fibers before (*a*) and after (*b*) a single TE pass

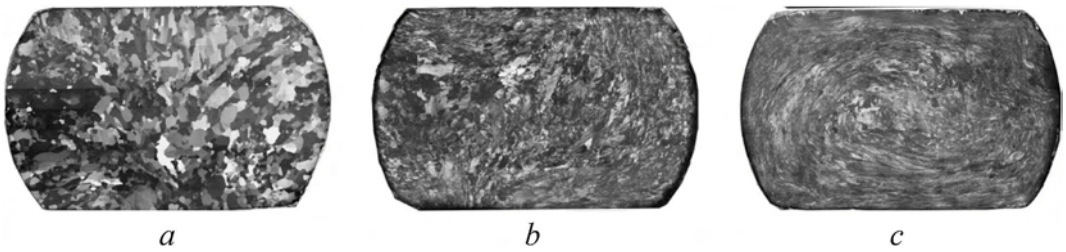

Fig. 8. Optical micrographs of cross-sections of 99.99% pure Al billets before TE (*a*), and after one (*b*) and four (*c*) TE passes

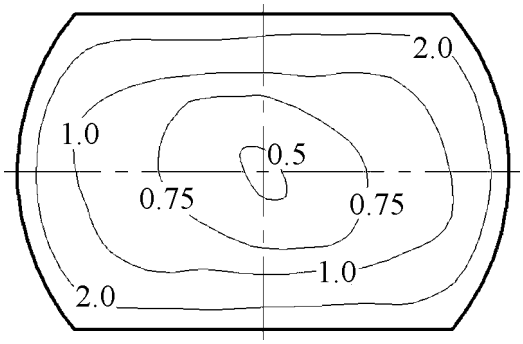

Fig. 9. Experimental distribution of von Mises equivalent strain in the cross-section of a Cu billet after a single TE pass

The second important finding was a discovery of plastic flow within the virtual cross-sectional layers first reported in [3,6,26]. It is obvious from the distortion of fibres during one TE pass illustrated in Fig. 7, reported in detail elsewhere [27,33].

After several passes of TE processing, this effect results in a very clear vortex-like flow pattern in a billet cross-section illustrated in Fig. 8. Further details can be found in refs [13,14,16].

The third improvement of the model in sub-section 2.1 made later is a quantifiable significant strain on the billet axis. Fig. 9 shows an example distribution in the cross-section of Cu billet after a single TE pass. It was obtained experimentally using a method described in detail in [27].

A final element code 'Deform-3D' was used to investigate the effect of strain hardening rate on net strain distribution after TE processing. The stress-strain curve of a material being processed was described by an equation $\sigma = \sigma_s (1 + Ae)$. Coefficient *A* was varied in the range [0–1] to simulate different rates of strain hardening.

Die and punches were modelled with rigid elements. Zibel law of friction $\tau = m\frac{\sigma_s}{\sqrt{3}}$ (where m = 0.25) was used in the simulations of contact on billet-die interface. Back pressure was set at a level sufficient to fill the die channel. Billet

material was modelled with tetrahedral elements. To accommodate large strains during simulations the adaptive meshing (automatic re-meshing) was used. Reduced integration and hourglass control were used in the analysis. Von Mises theory of plastic flow of incompressible materials was used. Geometry of the die used in simulations is shown in Fig. 10.

Fig. 11 illustrates the distribution of Von Mises equivalent strain in the billet cross-section after one TE pass. The distribution is shown with isolines for zero (A = 0) and maximal (A = 1) rates of strain hardening. Analysis of this figure reveals close similarity in the net strain distributions with small differences in its absolute values.

For the quantitative evaluation of Von Mises strain distribution after TE processing, we introduce the following criteria: minimum $e_{\min}$ and mean $e_{\text{mean}} = \frac{1}{S}\int_S e\mathrm{d}S$ strains as well as coefficient of strain heterogeneity $k_e = \frac{D_e}{e_{\text{mean}}}$, where D_e is standard deviation of Von Mises strain. Table 1 summarises values of these criteria for materials with the most representative values of strain hardening coefficient A.

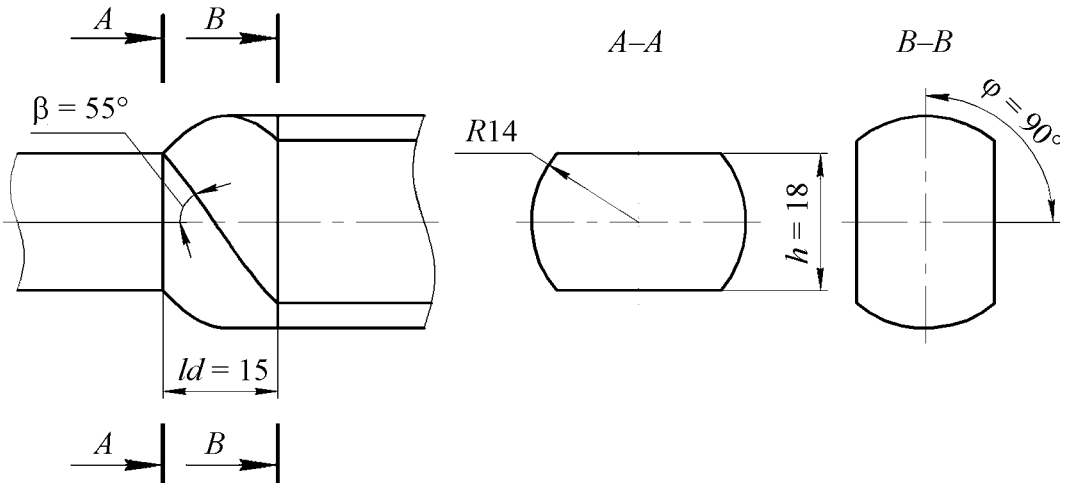

Fig. 10. Geometry of the die used in final element simulations (*A–A* – input cross-section, *B* – output cross-section)

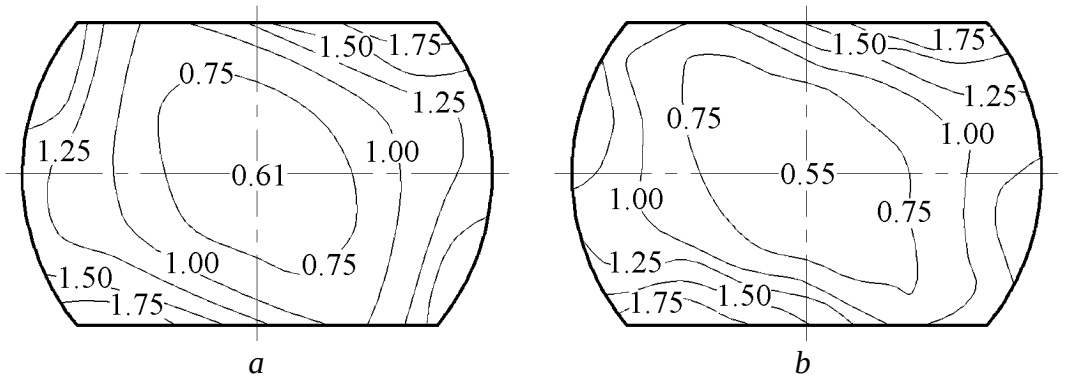

Fig. 11. Influence of rheology on accumulated von Mises strain after one TE pass of a material with zero, A = 0 (*a*), and maximal, A = 1 (*b*) rates of strain hardening

Table 1

Strain hardening dependencies of strain heterogeneity criteria in TE processing

A	$e_{\min}$	k_e	e_{mean}
0.0	0.61	0.27	1.00
0.5	0.64	0.28	1.07
1.0	0.55	0.33	1.07

These results clearly demonstrate that with the approximation sufficient for experimental practice, stress-strain state in TE processing can be simulated using ideally plastic model of a material being processed.

Fig. 12 demonstrates the accumulation of Von Mises equivalent strain during one TE pass in three representative points of a billet cross-section. Two zones of sharp strain growth corresponding to the inlet and the outlet from the helical part of the TE die can be easily located on the diagram for each point. Quantitative analysis of the strain accumulation reveals that the dominating mode of deformation in these zones is simple shear. In general, these results are in a reasonably good agreement with the simplistic model presented in subsection 2.1.

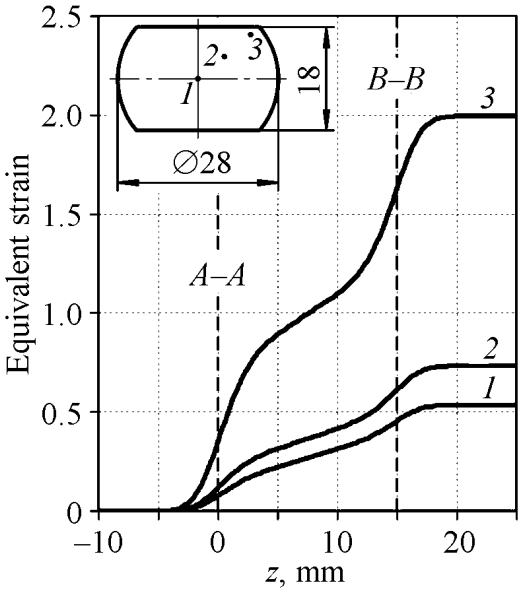

Fig. 12. Evolution of von Mises equivalent strain during one TE pass in three most representative points of a billet cross-section (*A–A* – input cross-section, *B–B* – output cross-section, see Fig. 10)

The final element simulations also reveal that the net strain distribution strongly depends on the shape of this cross-section, Fig. 13. In addition, this figure shows that for any cross-section profile, the minimum values of strain locate in the vicinity of extrusion axis.

When the axis of symmetry of cross-section profile coincides with the extrusion axis, multi-pass processing does not lead to the improvement of the net strain homogeneity. However, when these axes are shifted away from each other, the net strain homogeneity can be significantly improved if route II involving sequential change of CD and CCD dies is used for TE processing. Moreover, this technique allows to process by twist extrusion even the samples having circular profile of

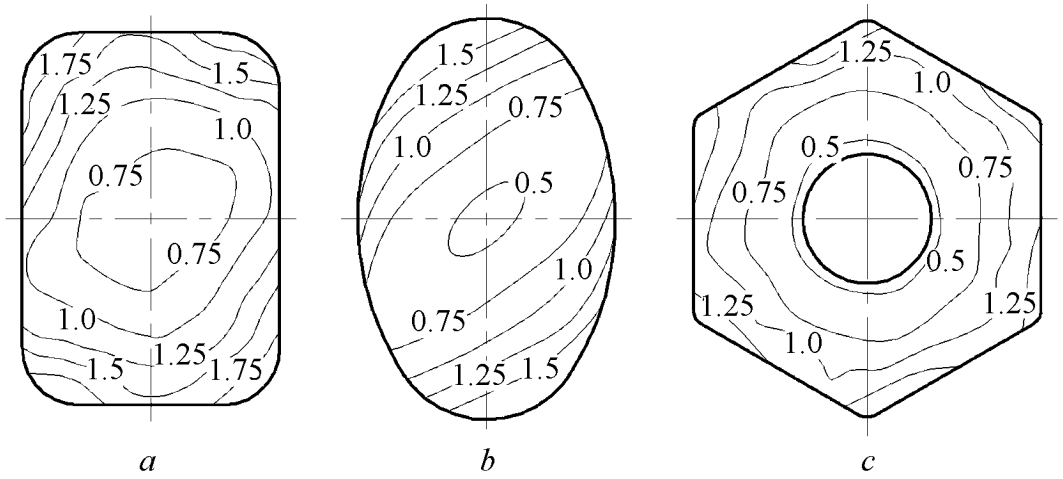

Fig. 13. Distributions of von Mises equivalent strain in cross-section of billets having rectangular (*a*), oval (*b*) and hexagonal with hollow centre (*c*) profiles

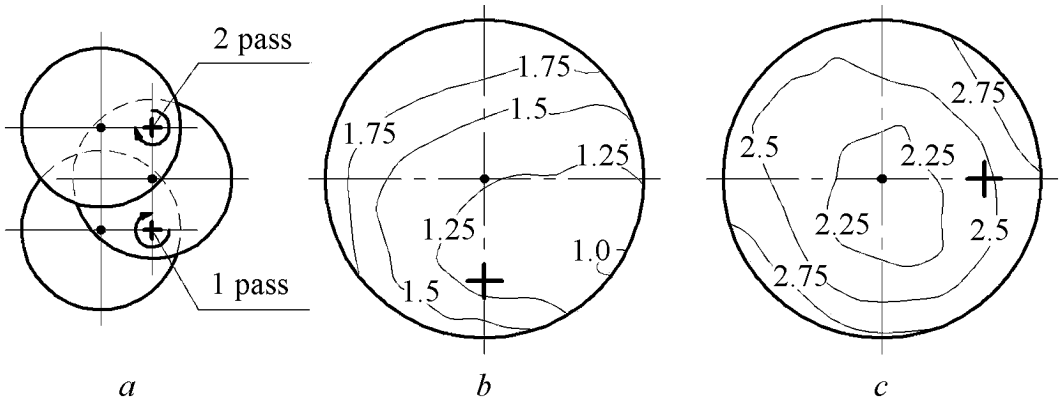

Fig. 14. Processing scheme where '•' and '+' indicate the axes of extrusion and the cross-section profile symmetry, respectively (*a*). Distribution of net strain in a billet having circular profile of cross-section after one (*b*) and two (*c*) TE passes by route II

cross-section. The net strain distribution for such a case is shown in Fig. 14. It is evident that homogeneity of the net strain distribution significantly improves after the second pass of TE, Fig. 14,*c*. If extrusion axis is shifted in each TE pass, rather homogeneous distribution of net strain can be achieved.

In the practice of twist extrusion, it is desirable to have as homogeneous distribution of strain along the specimen axis as possible. Our investigations prove that the best practice is achieved when both back pressure and dummy billets are used, i.e. when complete filling of cross-sectional profile of TE die channel is attained. This result is illustrated in Fig. 15 where distribution of net strain in longitudinal section of a prismatic billet is illustrated.

Stress state in TE can be classified as 'non-equiaxial compression'. Therefore full stress tensor can be split into hydrostatic and deviatory parts. The distributions of the hydrostatic stresses in billet cross-section on entrance and exit from the helical part of TE die are shown in Fig. 16. Large negative values of this characteristics ensure the best possible ductility in a material being processed [30].

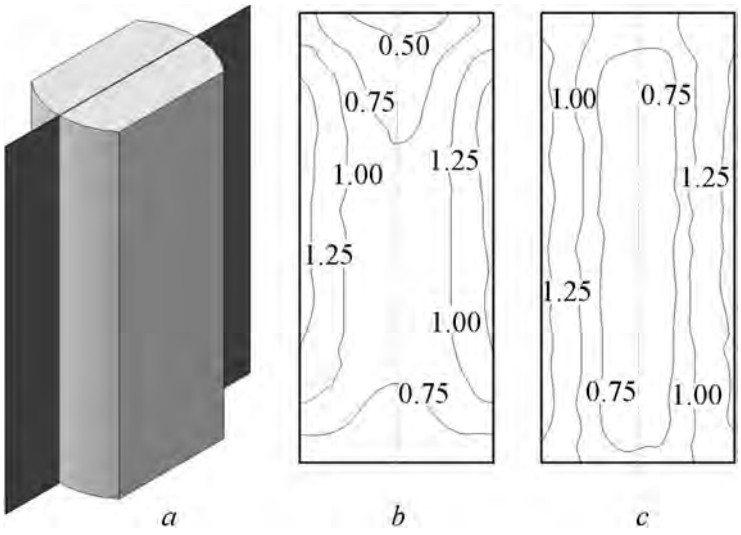

Fig. 15. Distribution of net strain in longitudinal section of a prismatic billet: *a* – schematic of the billet sectioning; *b* – isolevels of strain distribution in billets extruded without backpressure; *c* – with both backpressure and dummy billets

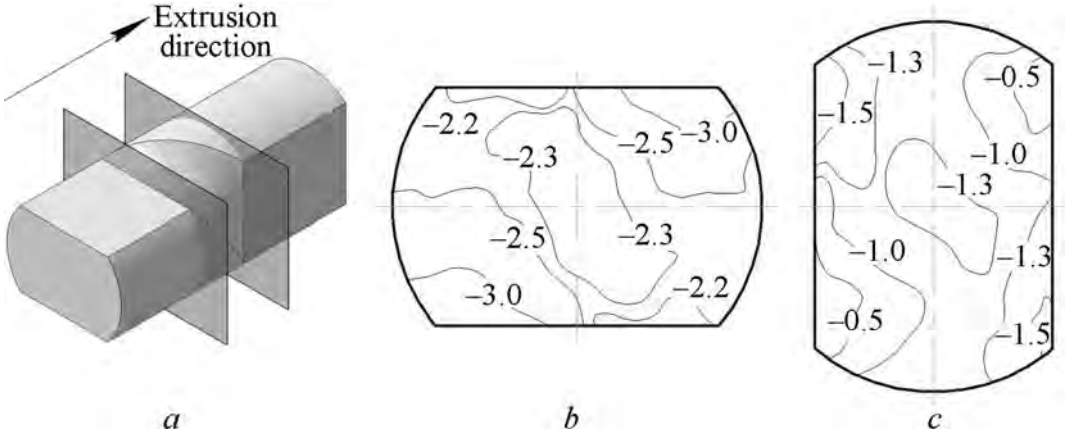

Fig. 16. Scheme of locations of indicative cross-sections in TE die (*a*) and distributions of hydrostatic stresses in billet cross-section on entrance (*b*) and exit (*c*) from the helical part of TE die. The isolevels show hydrostatic pressures normalized on flow stress of a material being deformed

3. Twist extrusion as a processing technique

In this subsection, equations for the calculation of main parameters of TE are presented, and a tool set for twist extrusion located in the pilot production facility of Donetsk Institute for Physics and Engineering of the National Academy of Sciences of Ukraine is described.

3.1. Principal equations for the estimation of processing characteristics

The development of a twist extrusion technology is based on the analysis of criteria characterising the process. In section 2, the following criteria describing homogeneity of strain distribution in TE have been introduced: minimum $e_{\min}$ and mean e_{mean} strains, and coefficient of strain heterogeneity k_e. In order to obtain simple engineering equations for these criteria, a series of numerical experiments was performed in final element code Deform–3D. The scheme of a channel in TE die for these experiments is shown in Fig. 17.

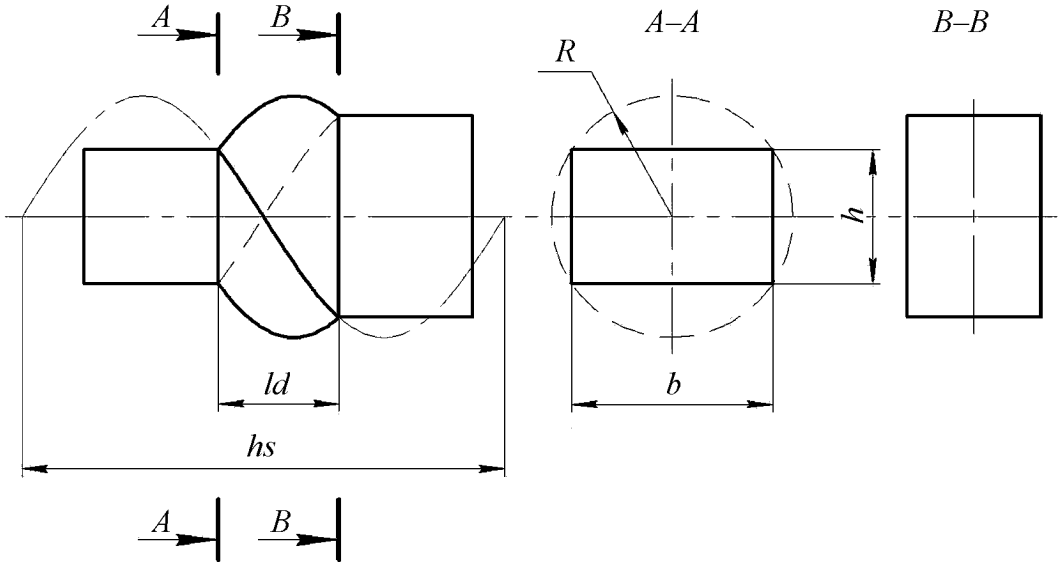

Fig. 17. Scheme of a channel in TE die for numerical experiments

The factors selected for variation are: $x_1 = hs/R$, $x_2 = ld/hs$, $x_3 = h/b$, where *hs*, *R*, *ld*, *h*, *b* are parameters of deformation zone indicated in Fig. 1. The ranges for these factors variation are selected from the following considerations. Based on the experience of experimental work with TE, reasonable values of twist line slope vary within β = 30–60°, angles of rotation between entrance and exit cross-sections are φ = 30–90°. Since $\tan\beta h_s = 2\pi R$, we obtain $x_1 = hs/R = 2\pi\beta$. Substituting the reasonable values for β, the range of variation for x_1 = 3–11. For x_2, we have $x_2 = ld/hs = \varphi/2\pi$, and the corresponding range of variation is x_2 = 0.10–0.25. The range of variation for x_3 = 0.5–1.0. All the factors were varied at three levels. The upper and lower levels were set by the ranges of variation, while the main level was set as arithmetic mean of the upper and lower levels.

Regression analysis of the results of numerical experiments allows obtaining the following equations for the calculation of the main criteria of TE processing:

$$e_{\min} = 3.08\left(\frac{hs}{R}\right)^{-0.65}\left(\frac{ld}{hs}\right)^{0.87}\left(\frac{h}{b}\right)^{-1.15}, \quad R^2 = 0.97, \tag{6}$$

$$k_e = 0.28\left(\frac{hs}{R}\right)^{-0.06}\left(\frac{ld}{hs}\right)^{-0.39}\left(\frac{h}{b}\right)^{076}, \quad R^2 = 0.87, \tag{7}$$

$$e_{\text{mean}} = 3.46\left(\frac{hs}{R}\right)^{-0.47}\left(\frac{ld}{hs}\right)^{0.55}\left(\frac{h}{b}\right)^{-0.56}, \quad R^2 = 0.93, \tag{8}$$

where R^2 is the coefficient of correlation.

Fig. 18 demonstrates the diagrams comparing the main criteria of TE processing obtained in numerical experiments to the values of these parameters calculated using equations (6)–(8).Very consistent fit of the experimental data with corresponding equations is obvious from these diagrams.

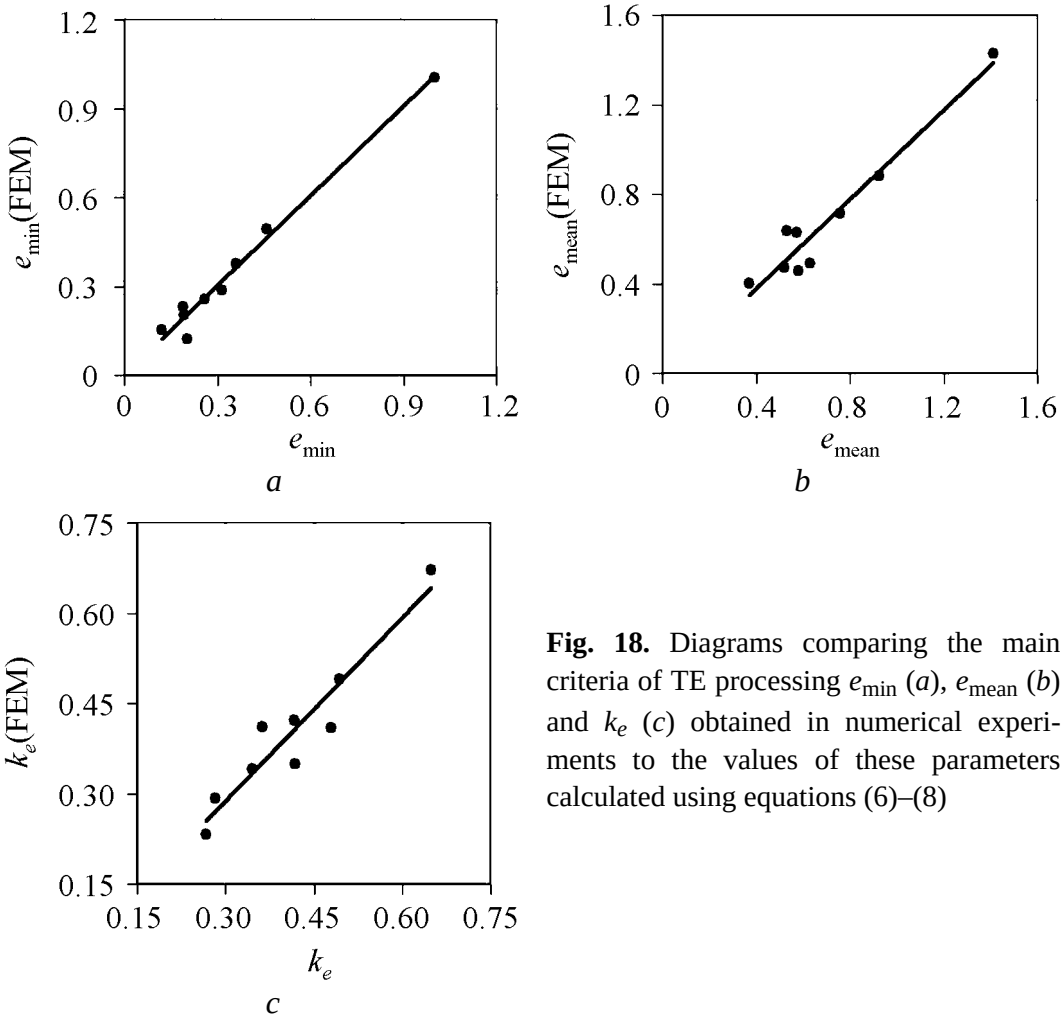

Fig. 18. Diagrams comparing the main criteria of TE processing $e_{\min}$ (*a*), e_{mean} (*b*) and k_e (*c*) obtained in numerical experiments to the values of these parameters calculated using equations (6)–(8)

Pressure for twist extrusion can be calculated using equation from [3]:

$$p_{\max} = \sigma\left(e_{\text{mean}} + \mu \frac{2(h+b)l}{hb} \right) + p_{bp}, \tag{9}$$

where σ is flow stress of a material being processed on the exit from TE die; l is the length of a billet, and p_{bp} is the back pressure.

3.2. Industrial prototype of twist extrusion machine

A pilot production facility has been created in Donetsk Institute for Physics and Engineering of the National Academy of Sciences of Ukraine. This facility has total area of 50 m^2 and includes:

– equipment for thermal and chemical treatments;

– furnace for billets pre-heat;

– hydraulic press having 4 MN extrusion force capacity on which toll sets for twist extrusion and hydro extrusion are installed;

– several machines for mechanical operations;

– other associated equipment.

Fig. 19 demonstrates drawing of a general assembly, Fig. 19,*a*, and a photograph, Fig. 19,*b*, of industrial prototype of twist extrusion machine in the pilot production facility. The main architectural units of this tool set are the upper movable ram *1* and the bottom base *2* of the press, container *3*, deforming TE die *3*, receiving container *5*, plunger *6*, back pressure plunger *7*, guide *8*, double-end bolts *9*, movable block *10*, wedge *11*, and back pressure hydro cylinder *12*.

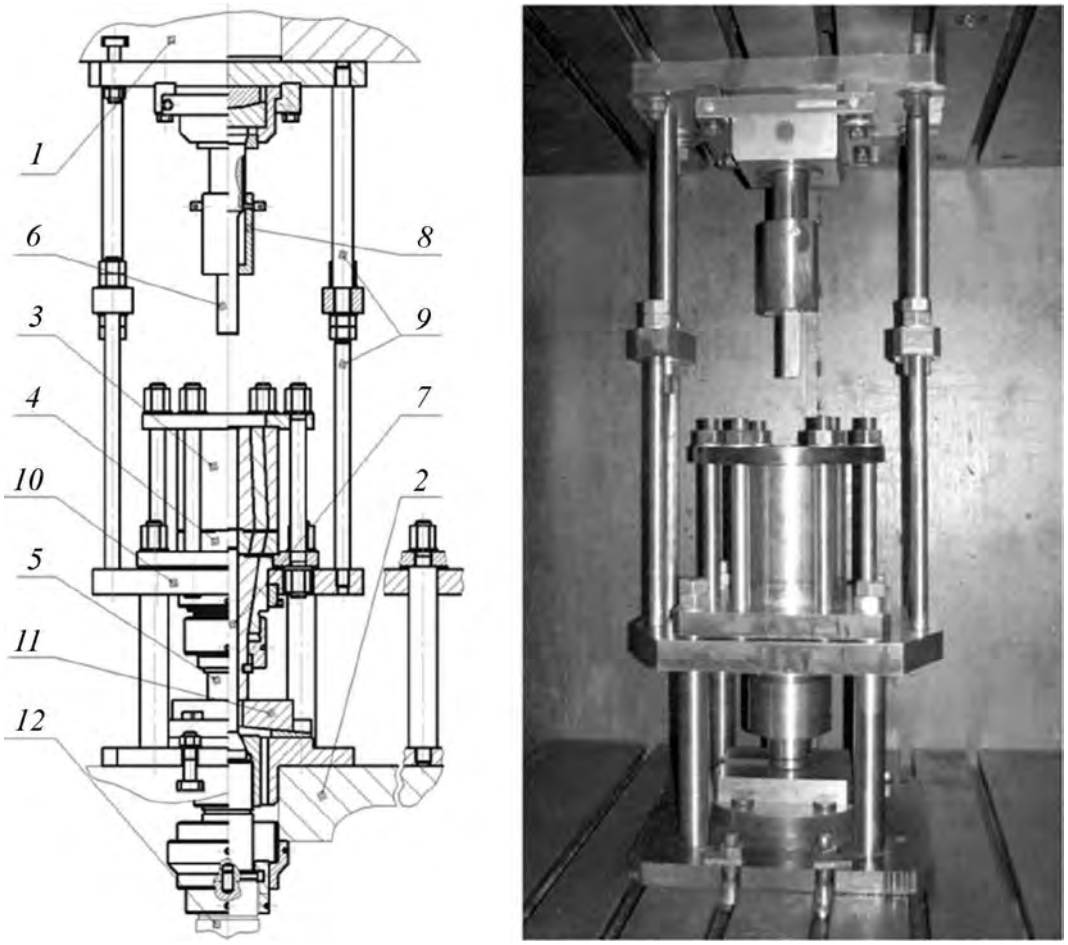

a *b*

Fig. 19. Industrial prototype of twist extrusion machine: *a* – the scheme of general assembly drawing, *b* – photograph of TE tool set

An operation cycle of the industrial prototype machine is shown in Fig. 20. The sequence is as follows. The receiving container is compressed to TE die by the upper ram, see Fig. 20,*a*. This action is realised by the moving block and the double-end bolts. The compression force is controlled by the hydraulic press. It is usually set to 0.2 MN. The position of the receiving container is set by the wedge. The back pressure plunger is inserted up to the exit section of the helical part of TE die through the channel of the receiving container.

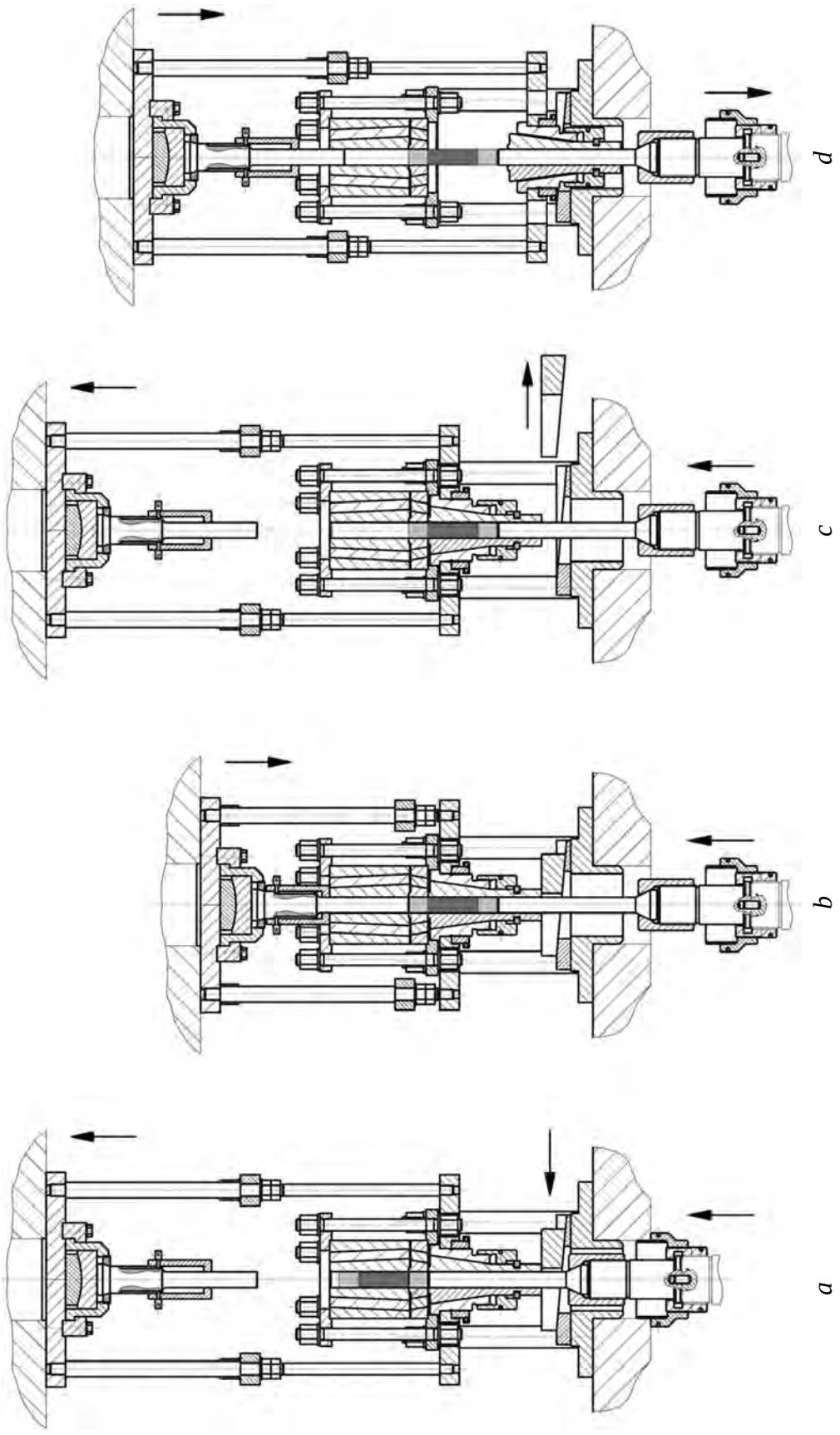

Fig. 20. Operation cycle of the industrial prototype machine for twist extrusion

A dummy billet is inserted in the container and pressed in to the helical part of TE die down to a contact with the back pressure plunger. The upper movable press ram is lifted up, and a billet to be processed having dimensions 30 × 40 × 140 mm is loaded in the container. After that, the upper dummy billet is loaded in the container in order to extrude out the billet from the helical part of TE die 'in one pass'.

Then, the ram starts moving down. During this operation, the plunger is centred by the guide first, and then it extrudes all the billets. The extrusion of the billets simultaneously gives rise of back pressure to a preset level. The later allows to satisfy the kinematic conditions of plastic flow and to largely increase the level of hydrostatic pressure in the deformation zone. High level of hydrostatic pressure minimises a loss of ductility in the billet and therefore permits processing of hard to deform materials.

The level of back pressure is usually set to the level of flow stress of a material being deformed at the temperature of processing. The back pressure plunger moves down therefore leaving behind room in the receiving container channel for the billets.

At the bottom point of the ram travel, the upper dummy billet replaces the initial dummy billet in the helical part of TE die, cf. Fig. 20,*b*. This allows doing multi-pass processing.

After this operation, the receiving container is compressed to TE die again, see Fig. 20,*c*, which unloads the wedge and allows its removal. During the working travel of the ram, the receiving container also moves down, Fig. 20,*d*. Therefore, at the end of extrusion operation, the back pressure plunger is moved down the channel, and the billets are extracted from the receiving container.

In order to process hard to deform materials, the entire tool set can be heated up by electric resistance heater.

To summarise, the industrial prototype tool set for twist extrusion is installed on a hydraulic press having the capacity of 4 MN. The installation has the following parameters:

– extrusion speed 3 mm/s;
–maximum extrusion force 2.4 MN;
– maximum back pressure force 2.4 MN;
– maximum operating temperature 400°C;
– billet size: cross-section 30 × 40 mm, length up to 140 mm.

4. Formation of structure and properties by twist extrusion. Experience and potential of the technique

The effects of processing by twist extrusion on the structure and the properties of miscellaneous materials have already been reported elsewhere rather well, e.g. [4,7,8,11–21, 23–25,33–35]. Therefore, in this section we will summarise the reported results, indicate the most representative data, and describe potential applications of TE technique.

4.1. Major effects of twist extrusion

First of all, intensive grain refinement during TE should be emphasised. The very process of grain refinement is not the topic of interest in the present chapter, and therefore readers are referred to specific publications dedicated to this problem, e.g. [36–39]. Briefly, grain refinement is characterised by a decrease in the grain size and an increase in misorientations on the boundaries when the equivalent Von Mises strain increases. In twist extrusion, grain refinement is very extensive during initial several passes. After the third or fourth pass, depending on a material being processed and processing conditions, the intensity of grain refinement substantially decreases, and the mean grain size saturates at the lowest level specific to the material. For processing at low homologous temperatures, the mean grain size at saturation stage is usually at the order of a few hundreds nanometres.

Second, the described characteristics of microstructure evolution largely affect also the mechanical properties of processed materials. Strain hardening decreases after the several initial passes, and the flow stress saturates, cf. [3,4,8,12,14,16,34,35]. Such behaviour leads to the homogenisation of mechanical properties in a billet after multi-pass TE processing [8,16,21]. Therefore, in spite of heterogeneity of net strain distribution described in previous section, the billets with ultrafine-grained (UFG) structure manufactured by twist extrusion have rather homogeneous mechanical properties.

In works [15,16,35], the effects of strain reversal in TE on microstructure evolution have been investigated experimentally. It has been shown that route II (CD + + CCD, subsection 2.1) is more efficient for grain refinement. This result is in consistency with theoretical investigation [40] according to which increase of deformation cycle amplitude should lead to more effective grain refinement.

Third, the effect of TE processing on ductility characteristics is of significant interest. Works [41,42] have shown that appropriate measure of ductility in UFG metals is reduction in area. This characteristic has non-monotonic strain dependence in TE. During several initial passes it decreases, but then increases. In [41], this effect has been shown for TE processing of Cp Ti. A mathematical model clarifying physical meaning of this effect has been developed in [40].

Finally, deformation during TE processing involves significant mass transfer taking place at different length scales of a material being processed. At a macro-scale level, the mass transfer is reflected by vortex-like plastic flow within billet cross-section, cf. subsection 2.2. At a micro-scale level, the mass transfer is reflected by dispersion of brittle intermetallic phases and abnormally fast diffusion, see for instance [3,24,43].

The fast mass transfer can be explained using the theory of two-stage simple shear [43–46]. At the first stage, in the range of shear strain $0 < \gamma < \gamma_c$ where γ_c is a parameter of a deformation process, the microstructure evolves in a way similar to elongation. At the second stage, when $\gamma > \gamma_c$, incidental multi-scale rotations take place in a way similar to turbulence in fluids. Physical reasons for such rotations are high pressure on shear plane, and asymmetry in stress tensor caused by the network of

high-angle grain boundaries permitting sliding. At the second stage, large plastic deformations on macro scale is realised through small cyclic elastic-plastic deformation of material particles inside a representative volume element. At this stage, extensive mass transfer takes place during rotations, deformation-induced dislocations move from sub grain interiors to their boundaries, and healing of nano-scale voids formed at earlier deformation stages. As a result, ductility of this metal increases.

The last but not the least, twist extrusion of powder materials results in a very efficient consolidation. Namely, compacting accompanied with formation of strong mechanical interlocking of particles takes place. This effect has been studied experimentally in [24,25,47,48]. The calculations of TE processing of non-solid materials based on a model developed in [49] have been reported in [48,50].

4.2. Applications of Twist Extrusion

Effects described in previous subsection 4.1 have different ways of application. The effect of grain refinement has been used for the manufacturing of nano- and UFG structured materials with improved mechanical properties. The homogenisation effect has been used for cast dendritic structure improvement and increase of ductility in recycled non-ferrous alloys. The powder consolidation effect has been used for consolidation of powders and machine chips. Each of these applications is described in detail below.

Applications Based on the Effect of Grain Refinement. By now, this effect has been used to manufacture UFG structured billets from Al–Mg-based alloys. The mean grain size after fourth TE pass was refined down to 300–500 nm, Fig. 21.

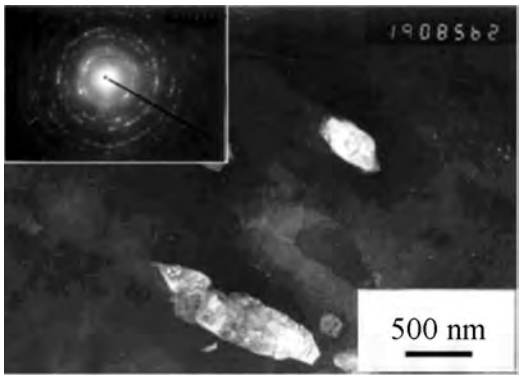

Fig. 21. Dark field TEM micrograph of microstructure in Al–Mg–Sc–Zr alloy manufactured by TE. SAED pattern is shown in the inset

The mechanical properties of this alloy are shown in Table 2. It can be seen that the material processed by four-pass TE was of higher ultimate tensile strength (UTS), approximately 20% improved yield strength (YS), and almost doubled fatigue strength (σ_{-1}). Such a material becomes an excellent candidate for utilisation in structural components of aircrafts and automobiles. The utilisation of this alloy should allow for weight savings reducing fuel consumption and increasing lifetime of a vehicle components.

Table 2

Mechanical properties of alloy Al–4.45Mg–0.4Mn–0.3Sc–0.1Zr (in wt.%)

Condition	YS	UTS	σ_{-1}	El, %
	MPa			
Initial	290	400	15	180
4 pass TE	350	420	10	330

Another material that has excellent perspectives in the application of TE based on grain refinement is commercially pure titanium (Cp Ti) for biomedical applications. Cp Ti (Grade 2) has been processed by TE for up to four passes and then rolled at ambient temperatures. As a result of such processing, microstructure in this material has been refined to sub-micron level, see micrograph in Fig. 22. Strength increased for two times, while elongation to failure (El) remained almost unchanged, see Table 3.

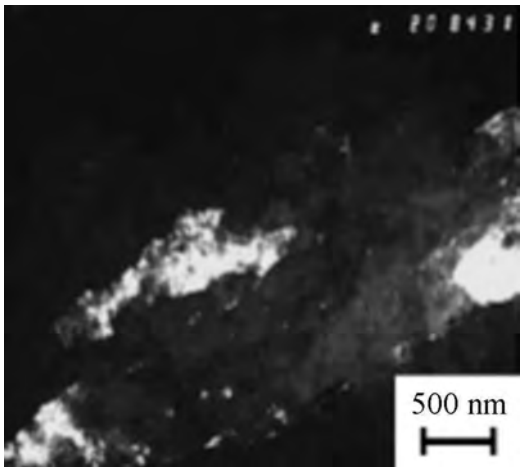

Fig. 22. Dark field TEM micrograph of microstructure in Cp Ti, Grade 2, after processing by four-pass TE

Table 3

Mechanical properties of Cp Ti, Grade 2

Condition	YS	UTS	El, %
	MPa		
Initial	350	430	20
4 pass TE + rolling 70%	800	840	15

The TE processed billets were used to machine plates for orthopaedic applications, a few examples of which are shown in Fig. 23. For such products, alloy Ti–6Al–4V modified for bio-medical applications is typically used. However, it has become possible to replace it with Cp Ti due to the improved mechanical properties. A benefit of using Cp Ti instead of Ti–6Al–4V is better biocompatibility due to the absence of vanadium (V) having toxic oxides and aluminium (Al) which may cause the Alzheimer's disease. In addition, due to the improved strength of UFG structured titanium, spectrum of implant shapes can be substantially increased, including the reduction of their dimensions.

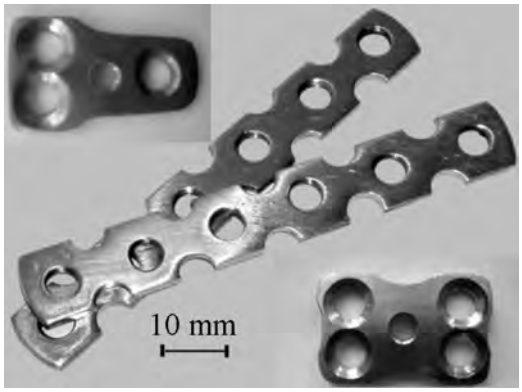

Fig. 23. Orthopedic plates from UFG titanium manufactured by TE

Applications Based on the Effect of Homogenization. Due to the vortex-like plastic flow in a billet cross-section and the stirring effect, TE provides intensive homogenization of alloys being processed. These effects have been applied for the processing of recycled non-ferrous metals and for the production of precision wires for fusion welding electrodes. As can be found in Table 4, both strength and ductility of the recycled alloys were enhanced after processing by TE for homogenization.

Table 4

Mechanical properties of recycled non-ferrous alloys before and after processing by TE for homogenization

Main elem. content	Initial state				After TE			
	UTS	YS	El	RA	UTS	YS	El	RA
	MPa		%		MPa		%	
Al 99.3%	96.5	84	11	17	159	137	21	70
Al 98.0%	99	81	10	15	299	263	14	30
Al 88% Si 9.5%	75.2	60	1.5	0	203	180	12	13
Al 93% Mg 2.28%	62	60	1.5	1	324	269	3.8	11
Cu 81% P 9%	–	300	1	–	–	420	11	–

The simultaneous improvement of both strength and ductility characteristics is explained by the dispersion of brittle intermetallics populated along grain boundaries, which is typical for these alloys, see Fig. 24.

The significant improvement of ductility in these alloys after TE processing made possible further forming by plastic deformation. Hence, the final products, illustrated in Fig. 25, have been manufactured by following hydro extrusion. Summarising these results, let us note that the processing of as-cast recycled non-ferrous metals by TE for homogenisation also allows to increase both the spectrum of the final products and the added value of these alloys by making them suitable for further forming.

Applications Based on the Effect of Powder Consolidation. Until now, this effect has been used for the manufacturing of long bars from magnesium (Mg), copper (Cu), and Al machine chips. For this purpose, an integrated tool set combining TE die followed by conical die schematically shown in Fig. 26 has been used.

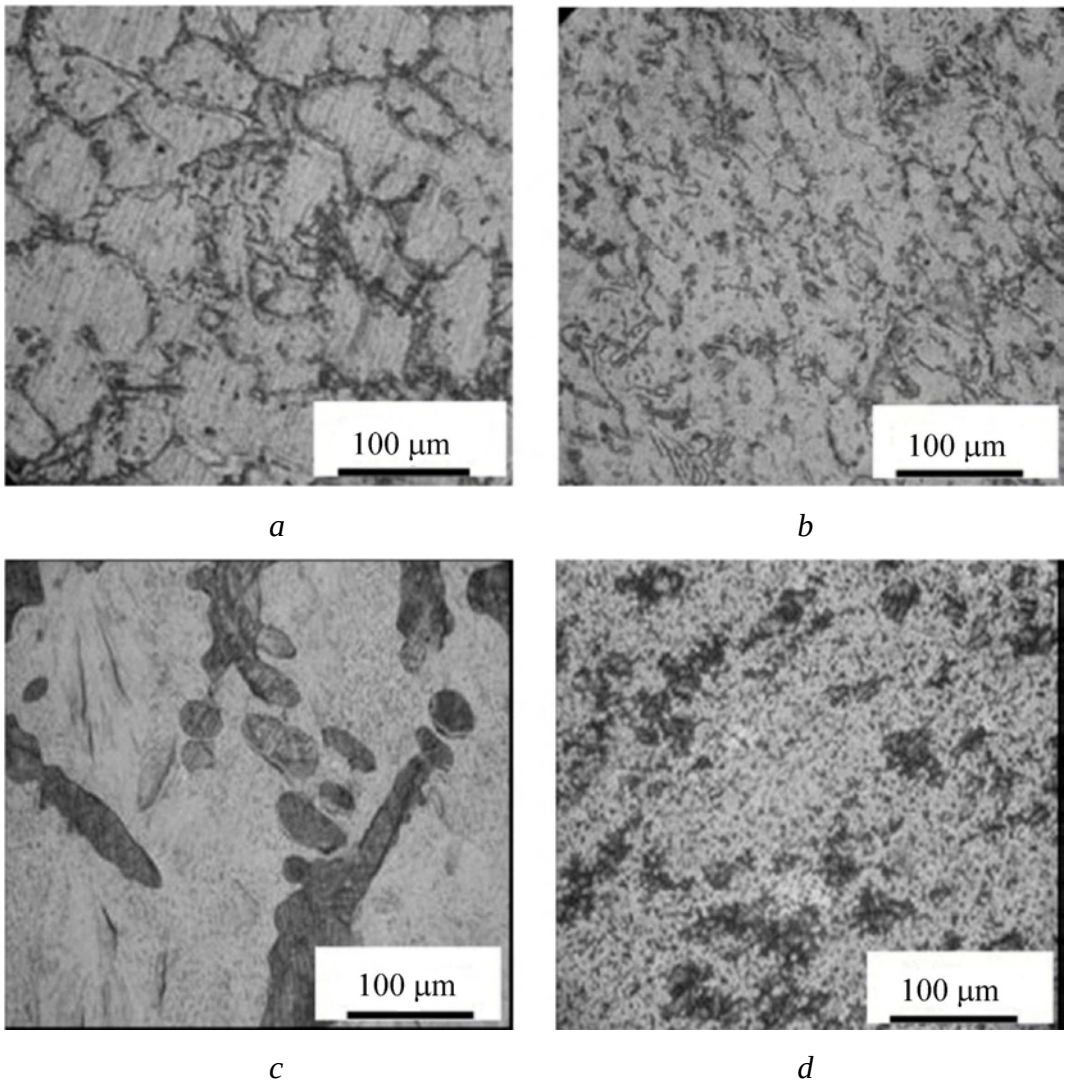

Fig. 24. Homogenization of Al (*a*, *b*) and Cu-based (*c*, *d*) recycled alloys: *a*, *c* – initial as-cast microstructure; *b*, *d* – after TE processing

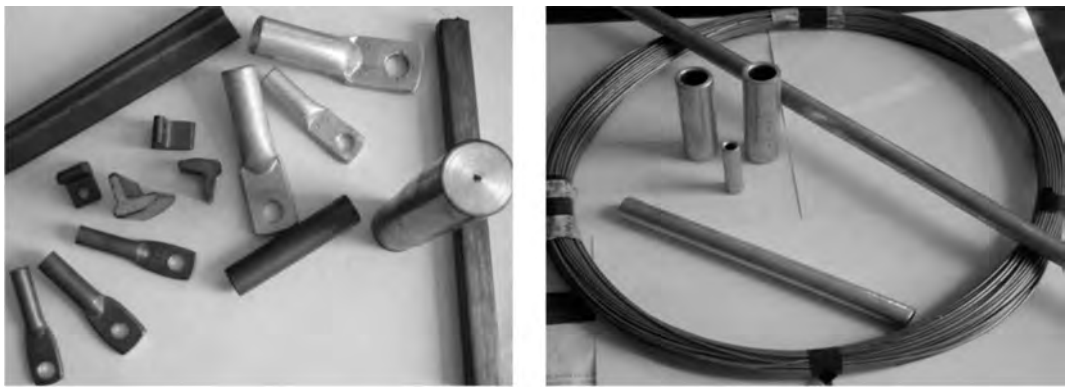

Fig. 25. Final products from recycled non-ferrous metals manufactured by TE processing and following extrusion

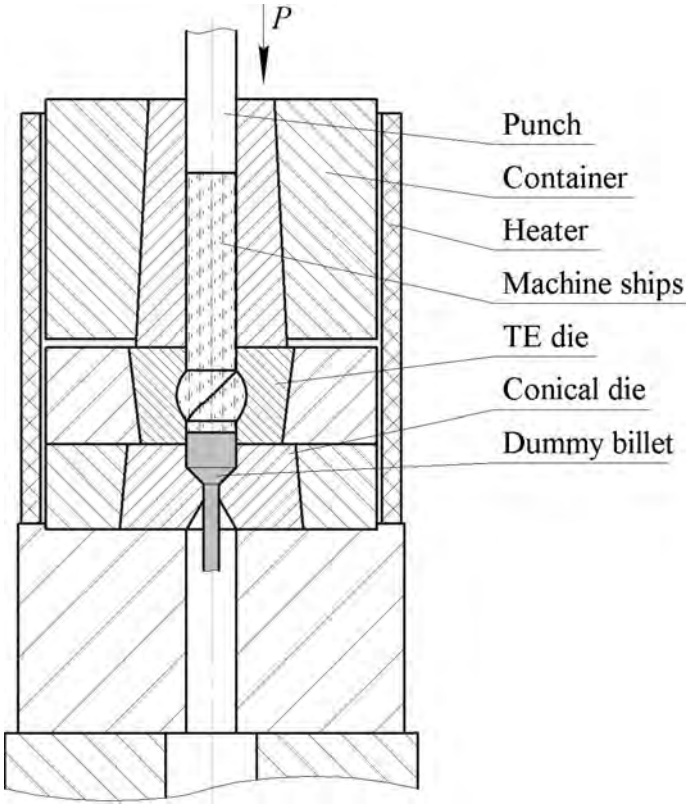

Fig. 26. Schematic of integrated tool set combining TE die followed by conical die for the consolidation of powders

Using this tool set, rods of 10–15 mm in diameter and up to 1 m in length have been manufactured in a single pass from machine chips. Mechanical properties of these rods are similar to those in solid rods obtained in a traditional way.
The tool set shown in Fig. 26 has also been used for the consolidation of titanium sponge into electrodes for electro slag re-melting.

5. Recent developments in twist extrusion and its derivatives

Recently two new prototypes based on twist extrusion concept have been developed. We believe these prototypes have excellent perspectives for industrial applications and therefore describe them in this section. The first one is a planar twist extrusion (PTE), which allows processing of long billets with large width-to-thickness ratio of cross-section [32,51]. The second one is a laboratory horizontal tool set for twist extrusion, which allows manufacturing of composite and gradient materials.

5.1. Planar twist extrusion

The size of a billet for TE is limited by two factors: (i) aspect ratio (length/diameter) has to be smaller than a critical value to avoid bending of a plunger during extrusion, and (ii) the plunger has a limited travel distance. These are principal limitations imposed by the processing scheme such as extrusion. In the case of traditional extrusion, this is acceptable since a billet being extruded experiences significant elongation during processing. However, in the case of SPD processing based on the extrusion scheme, e.g. ECAE etc., these limitations

become a significant drawback since the net shape of billets remains unchanged after processing.

Such a drawback can be overcome by the application of two-sided gripping of feedstock, for instance Linear Continuous Extrusion (LINEX) [52], as well as by using containers and dies with movable walls. The later option permits control of magnitude and direction of frictional forces on the billet-tool interface, reduces pressure applied to the plunger by partial transfer of load onto the movable die walls, and allows to design the plunger as a more stable and stronger component. In [53], Segal proposed design of a unique ECAE tool set in order to reduce the frictional forces. In this tool set, three lateral sides of a billet are surrounded by the plunger, and the bottom side of the die channel is free to move.

Unfortunately, this concept of tool design cannot be directly applied to TE, as the die channel has helical, i.e. non-flat, lateral surfaces. Therefore, twist extrusion with two parallel die walls named Planar Twist Extrusion, has been proposed in [51]. Later, the same scheme was proposed by Pardis et al under the name ‘simple shear extrusion’, e.g. [54]. As can be found in Fig. 27, the primary difference between TE and PTE is the shape of deforming zones in corresponding dies. In TE, all four walls of the die have the same helical shape, while in PTE only two opposite walls of the die are ruled surfaces, while the other two are flat and parallel to each other.

As can be seen in Fig. 27,*a*, PTE die channel has three distinct segments. Namely, these are straight entry and exit segments with rectangular cross-section separated by deforming one in between. The deforming segment has cross-section varying along the die axis from rectangular to parallelogram and then back to rectangular, Fig. 27,*c*. The non-flat walls on this segment are ruled surfaces formed by moving a straight line along two directrices made by two straight segments conjugated with arcs, Fig. 27,*a*. Further details on such a surface geometry can be found in [55].

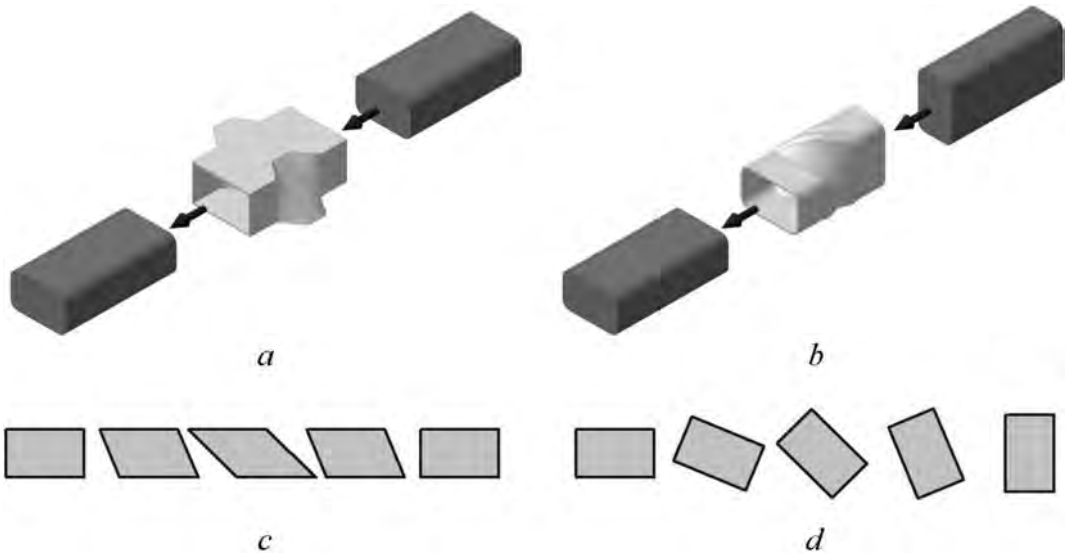

Fig. 27. Schematics of (*a*) PTE and (*b*) TE die channels; sequential cross-sections of the die channel for (*c*) PTE and (*d*) TE

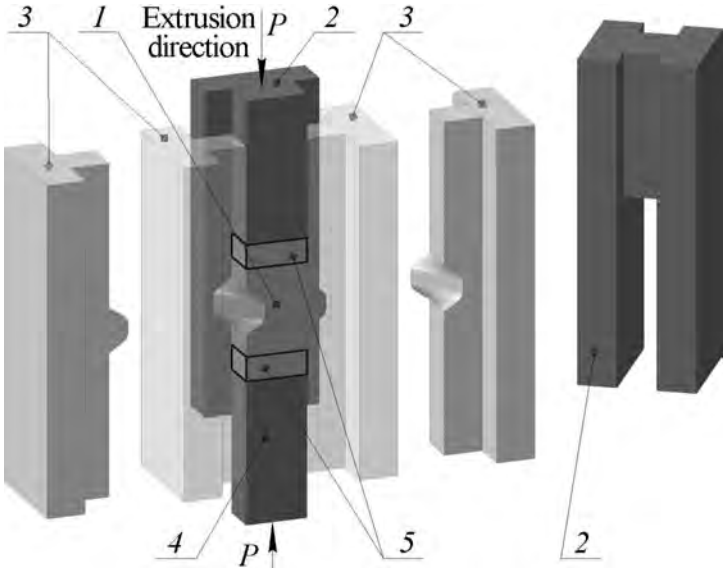

Fig. 28. PTE die with two flat movable walls: *1* is billet being processed, *2* – main plunger, *3* – curved stationary walls, *4* – back pressure plunger, *5* – dummy billets

In [32], planar twist extrusion has been investigated using a tool set with two flat movable walls, Fig. 28. In PTE, billet *1* is pushed by plunger *2* through the die channel formed by two curved *3* and two flat walls. The later is made as a single part together with the plunger. At the place of loading, the plunger has h-beam cross-section with an area larger than cross-section of the billed being extruded. This feature allows to improve the stability of the plunger and to increase the billet length. Load from main *2* and back pressure *4* plungers is transferred to the billet through two dummy billets *5*. Back pressure is necessary for the billet to fill the die channel entirely. In addition, this pressure increases hydrostatic pressure in the deformation zone, thereby improving ductility and promoting grain refinement [40].

Investigations in Ref. [32] revealed that although equivalent Von Mises strain accumulated after one pass can be the same on average in both PTE and TE processes, its distribution is substantially different depending on the processing technique. In PTE, isolevels of strain contours are elongated along the shorter side of rectangular cross-section of the billet, while in TE the contours are arranged into loops around the centre of the billet cross-section.

Recently, planar twist extrusion has been successfully applied for the processing of polymers [56].

5.2. Laboratory horizontal tool set for twist extrusion

Schematic of horizontal tool set for twist extrusion and its deforming parts are shown in Fig. 29. Principal novelty of such a tool set is split-design TE die. Its parts are compressed to each other during extrusion pass by a hydro cylinder.

When a billet being processed is inside, TE die can be split in two parts only if a perpendicular dropped from any point of the die surface on the jointing plane nowhere crosses the die body. Let’s obtain a mathematical equation for this condition.

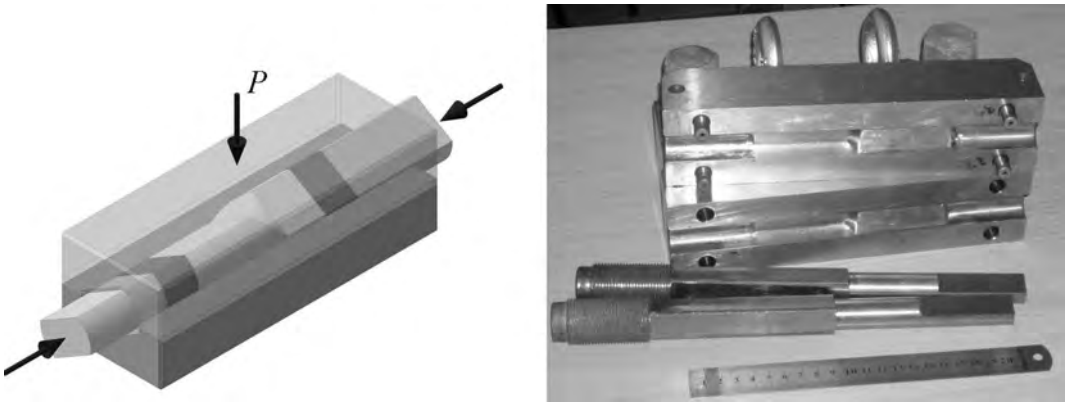

a *b*

Fig. 29. Scheme (*a*) and a photograph (*b*) of principal parts of horizontal tool set for twist extrusion

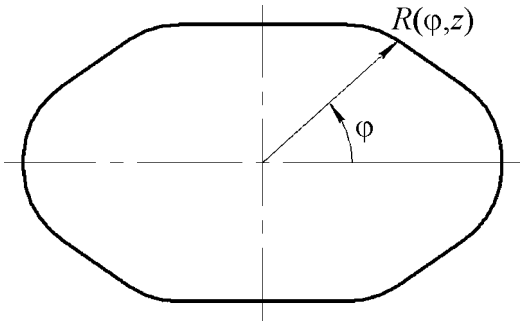

Fig. 30. Cross-section of split channel of TE die in section $z = 0$

In a cylindrical coordinate system (r, φ, z), where z axis is elongated with TE die axis, $r = R(\varphi)$ is the equation describing the contour of the die channel in cross-section $z = 0$. The jointing plane is defined by conditions $\varphi = 0$ and $\varphi = \pi$ as shown in Fig. 30.

The contour is considered smooth, i.e. function $R(\varphi)$ is continuous along with derivative $\frac{\mathrm{d}R(\varphi)}{\mathrm{d}\varphi}$ in the entire range of $0 \le \varphi \le 2\pi$.

The contour of the die channel in section z is the same as the contour in section $z = 0$, just rotated through the angle of $\alpha = 2\pi\frac{z}{h}$, where h is the twist line increment. Hence, the equation describing the contour of the die channel in section z will be:

$$r = R\left(\varphi - 2\pi\frac{z}{h}\right). \tag{10}$$

From Fig. 30, the aforementioned condition of TE die split is equivalent to the following:

$$\begin{cases} 0 \le \varphi < \pi, & \dfrac{\mathrm{d}\left(R\cos\varphi\right)}{\mathrm{d}\varphi} \le 0 \\ \pi \le \varphi \le 2\pi, & \dfrac{\mathrm{d}\left(R\cos\varphi\right)}{\mathrm{d}\varphi} \ge 0 \end{cases}. \tag{11}$$

From (11) one can obtain:

$$\begin{cases} 0 \le \varphi < \pi, & \dfrac{\mathrm{d}R}{\mathrm{d}\varphi}\cos\varphi \le R\sin\varphi \\ \pi \le \varphi \le 2\pi, & \dfrac{\mathrm{d}R}{d\varphi}\cos\varphi \ge R\sin\varphi \end{cases}. \tag{12}$$

From condition (12), on the jointing plane we have:

$$\frac{\mathrm{d}R}{\mathrm{d}\varphi} = 0\,. \tag{13}$$

In this case, from equation (10), on the jointing section:

$$\frac{\partial R}{\partial z} = 0\,. \tag{14}$$

Conditions (13) and (14) mean that in order to make TE die splittable when the billet being processed is inside, the parts of its channel contour on jointing plane should belong to a circular cylindrical surface.

In the tool sets for horizontal TE, the billet being processed is sequentially extruded through the die in both forward and backward directions. Two hydro cylinders located on both sides of the die work by turns acting either as the main or back pressure. This allows the processing of billets in conditions controllable by temperature, backpressure, strain rate, etc.

A number of tool sets for horizontal TE have been designed based on this scheme, two of which are shown in Fig. 31.

Conclusion

In the present paper, TE has been introduced as a unique technique for plastic deformation processing. Mechanics of plastic deformation in TE is thoroughly discussed, and simple engineering equations for the calculation of process parameters are proposed.

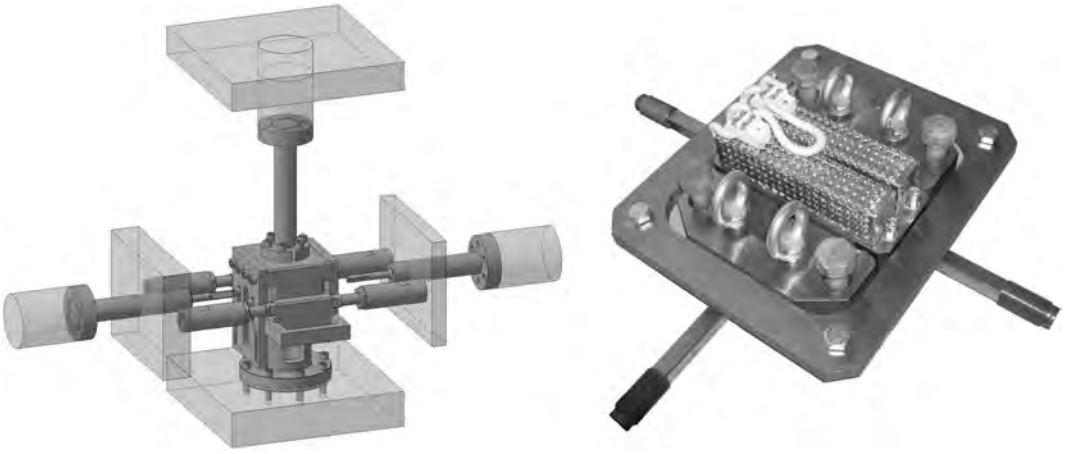

Fig. 31. Scheme (*a*) and a photograph (*b*) of tool sets for horizontal twist extrusion designed for Monash University (Melbourne, Australia) and University Paul Verlaine (Metz, France), respectively

Similar to the most widely used severe plastic deformation techniques HPT and ECAE, dominant deformation mode in TE is simple shear. However, due to unique properties of TE process, it opens extra options for materials engineering.

The effectiveness of TE processing for microstructure and property tailoring in metallic materials such as Ti alloys, super alloy Inconel 718; Al–Mg–Sc alloys; and recycled grades of Cu and Al alloys is illustrated.

At the moment, three directions of applications of TE processing can be highlighted:

– manufacturing of bulk nano-structured materials through grain refinement;

– manufacturing of bulk nano-structured materials through powders consolidation;

– improvement of ductility and microstructure homogenisation in recycled non-ferrous alloys due to vortex-like plastic flow in TE.

Most recent developments in tool design for twist extrusion and its derivatives are described.

The authors would like to many thanks PhD S. Synkov, Dr.Sc., PhD E. Pashinskaya and Eng. A.N. Sapronov without which the development of the twist extrusion in Donetsk Institute for Physics and Engineering of National Academy of Sciences of Ukraine would be impossible.

1. *Y.Y. Beygelzimer, V.N. Varyukhin, S.G. Synkov, A.N. Sapronov, V.G. Synkov*, Fiz. Tekh. Vys. Davl. **9**, № 3, 109 (1999).
2. *P.W. Bridgman*, Studies in large plastic flow and fracture, McGraw-Hill, New York, NY, USA (1952).
3. *Y. Beygelzimer, V. Varyukhin, D. Orlov, S. Synkov*, Twist extrusion – process for strain accumulation, TEAN, Donetsk (2003).
4. *V.V. Stolyarov, Y.E. Beigel'zimer, D.V. Orlov, R.Z. Valiev*, Phys. Metal. Metall. **99**, 204 (2005).
5. *Y. Beygelzimer, V. Varyukhin, D. Orlov, B. Efros, V. Stolyarov, H. Salimgareyev*, in: 2002 TMS Annual Meeting and Exhibition, TMS (The Minerals, Metals & Materials Society), Y.T. Zhu, T.G. Langdon, R.S. Mishra, S.L. Semiatin, M.J. Saran, T.C. Lowe (eds.), Seattle, Washington, USA, 2002, pp. 43–46.
6. *D. Orlov*, in: Department of metal forming, Donetsk National Technical University, Donetsk (2003), p. 172.
7. *D.V. Orlov, V.V. Stolyarov, H.S. Salimgareyev, E.P. Soshnikova, A.V. Reshetov, Y.Y. Beygelzimer, S.G. Synkov, V.N. Varyukhin*, in: 2004 TMS Annual Meeting, TMS (The Minerals, Metals & Materials Society), Y.T. Zhu, T.G. Langdon, R.Z. Valiev, S.L. Semiatin, D.H. Shin, T.C. Lowe (eds.), Charlotte, North Carolina, USA, 2004, pp. 457–462.
8. *Y. Beygelzimer, D. Orlov, A. Korshunov, S. Synkov, V. Varyukhin, I. Vedernikova, A. Reshetov, A. Synkov, L. Polyakov, I. Korotchenkova*, Solid State Phenom. **114**, 69 (2006).
9. *D. Orlov, A. Reshetov, A. Synkov, V. Varyukhin, D. Lotsko, O. Sirko, N. Zakharova, A. Sharovsky, V. Voropaiev, Y. Milman, S. Synkov*, in: Nanostructured Materials by

High-Pressure Severe Plastic Deformation, Y. Zhu, V. Varyukhin (eds), Springer Netherlands, 2006, pp. 77–82.
10. *V. Varyukhin, Y. Beygelzimer, S. Synkov, D. Orlov*, Mater. Sci. Forum. **503–504**, 335 (2006).
11. *M. Berta, D. Orlov, P.B. Prangnell*, Int. J. Mater. Res. **98**, 200 (2007).
12. *D. Orlov, Y. Beygelzimer, S. Synkov, V. Varyukhin, Z. Horita*, Mater. Trans. **49**, 2 (2008).
13. *D. Orlov, Y. Beygelzimer, S. Synkov, V. Varyukhin, N. Tsuji, Z. Horita*, Mater. Trans. **50**, 96 (2009).
14. *D. Orlov, Y. Beygelzimer, S. Synkov, V. Varyukhin, N. Tsuji, Z. Horita*, Mater. Sci. Eng. **A519**, 105 (2009).
15. *D. Orlov, Y. Todaka, M. Umemoto, Y. Beygelzimer, Z. Horita, N. Tsuji*, Mater. Sci. Forum. **604–605**, 171 (2009).
16. *D. Orlov, Y. Todaka, M. Umemoto, Y. Beygelzimer, N. Tsuji*, Mater. Trans. **53**, 17 (2012).
17. *V. Varyukhin, Y. Beygelzimer, B. Efros*, Mater. Sci. Forum. **584–586**, 102 (2008).
18. *Y. Beygelzimer, V. Varyukhin, S. Synkov, D. Orlov*, Mater. Sci. Eng. **A503**, 14 (2009).
19. *S.R. Bahadori, S.A.A. Akbari Mousavi, A.R. Shahab*, Journal of Physics: Conference Series **240**, 012132 (2010).
20. *V. Stolyarov, E. Pashinskaya, Y. Beigel'zimer*, Russ. Metall. **2010**, 904 (2010).
21. *A. Reshetov, A. Korshunov, A. Smolyakov, Y. Beygelzimer, V. Varyukhin, I. Kaganova, A. Morozov*, Mater. Sci. Forum. **667–669**, 851 (2011).
22. *V. Varyukhin, Y. Beygelzimer, R. Kulagin, O. Prokof'eva, A. Reshetov*, Mater. Sci. Forum. **667–669**, 31 (2011).
23. *H. Zendehdel, A. Hassani*, Materials & Design **37**, 13 (2012).
24. *A. Shevelev, Y. Beygelzimer, V. Varyukhin, S. Synkov, L. Ryabicheva, A. Reshetov*, Metal forming of the recycled aluminum and aluminum-containing alloys, Noulidzh, Donetsk (2010).
25. *A.P. Shpak, V.N. Varyukhin, V.I. Tkatch, V.V. Maslov, Y.Y. Beygelzimer, S.G. Synkov, V.K. Nosenko, S.G. Rassolov*, Mater. Sci. Eng. **A425**, 172 (2006).
26. *Y. Beygelzimer, D. Orlov, V. Varyukhin*, in: 2002 TMS Annual Meeting and Exhibition, TMS (The Minerals, Metals & Materials Society), Y.T. Zhu, T.G. Langdon, R.S. Mishra, S.L. Semiatin, M.J. Saran, T.C. Lowe. (eds.), Seattle, Washington, USA (2002), pp. 297–304.
27. *Y. Beygelzimer, A. Reshetov, S. Synkov, O. Prokof'eva, R. Kulagin*, J. Mater. Process. Tech. **209**, 3650 (2009).
28. *Y.Y. Beygelzimer, V.N. Varyukhin, V.G. Synkov, S.G. Synkov*, Fiz. Tekh. Vys. Davl. **24**, № 2, 10 (2000).
29. *M.I. Latypov, I.V. Alexandrov, Y.E. Beygelzimer, S. Lee, H.S. Kim*, Computational Materials Science **60**, 194 (2012).
30. *Y. Beygelzimer, D. Orlov*, Defect. Diffus. Forum **208–209**, 311 (2002).
31. *S.A.A. Akbari Mousavi, A.R. Shahab, M. Mastoori*, Materials & Design **29**, 1316 (2008).
32. *Y. Beygelzimer, D. Prilepo, R. Kulagin, V. Grishaev, O. Abramova, V. Varyukhin, M. Kulakov*, J. Mater. Process. Tech. **211**, 522 (2011).
33. *A. Reshetov*, in: Department of metal forming, Donetsk National Technical University, Donetsk, 2007.

34. *S.R. Bahadori, S.A.A.A. Mousavi*, Mat. Sci. Eng. **A528**, 6527 (2011).
35. *J. Gubicza, S.V. Dobatkin, E. Khosravi, A.A. Kuznetsov, J.L. Lábár*, Mater. Sci. Eng. **A528**, 1828 (2011).
36. *D.A. Hughes, N. Hansen*, Acta Mater. **45**, 3871 (1997).
37. *D. Kuhlmann-Wilsdorf, N. Hansen*, Scripta Metall. Mater. **25**, 1557 (1991).
38. *D. Orlov, N. Kamikawa, N. Tsuji*, Philos. Mag. **92**, 2329 (2012).
39. *V.V. Rybin*, Large plastic deformation and fracture of metals, Metallurgia, Moscow (1986).
40. *Y. Beygelzimer*, Mech. Mater. **37**, 753 (2005).
41. *Y. Beygelzimer, O. Prokof'eva, R. Kulagin, V. Varyukhin, S. Synkov*, Mater. Sci. Forum. **633–634**, 223 (2010).
42. *O. Bouaziz*, Mater. Sci. Forum. **633–634**, 205 (2010).
43. *Y. Beygelzimer*, Mater. Sci. Forum. **683**, 213 (2011).
44. *Y. Beygelzimer, R.Z. Valiev, V. Varyukhin*, Mater. Sci. Forum. **667–669**, 97 (2011).
45. *Y. Beygelzimer*, Fiz. Tekh. Vys. Davl. **20**, № 4, 40 (2010).
46. *Y. Beygelzimer*, Fiz. Tekh. Vys. Davl. **20**, № 1, 26 (2010).
47. *Y.E. Beygelzimer, O.V. Mikhailov, A.S. Synkov, M.B. Shtern, E. Olevsky*, Fiz. Tekh. Vys. Davl. **18**, № 1, 69 (2008).
48. *A. Synkov*, in: Department of metal forming, Donetsk National Technical University, Donetsk (2011).
49. *J.E. Beigelzimer, B.M. Efros, V.N. Varyukhin, A.V. Khokhlov*, Engineering Fracture Mechanics **48**, 629 (1994).
50. *Y. Beygelzimer, D. Prilepo, S. Synkov*, Fiz. Tekh. Vys. Davl. **17**, № 2, 100 (2007).
51. *W.G. Voorhes*, in: USPTO (Ed.) USPTO, Wanskuck Company (Providence, RI), USA (1975), pp. 1–6.
52. *V. Segal*, in: U.S. Patent (Ed.) USPTO, USA (1996), pp. 1–6.
53. *N. Pardis, R. Ebrahimi*, Mater. Sci. Eng. **A527**, 355 (2009).
54. *D. Hilbert, S. Cohn-Vossen*, Geometry and the Imagination, 2 ed., AMS Chelsea Publishing, Providence, R.I. (1999).
55. *V. Beloshenko, Y. Beygelzimer, V. Varyukhin*, Solid phase extrusion of polymers, Naukova dumka, Kiev (2008).

Я. Бейгельзимер, В. Варюхин, Р. Кулагин, Д. Орлов

ВИНТОВАЯ ЭКСТРУЗИЯ: ОБЗОР

Представлен обзор исследований по винтовой экструзии (ВЭ), выполненных в ДонФТИ начиная с 1999 г. Показано, что ВЭ имеет значительный коммерческий потенциал в связи со следующими физическими эффектами: интенсивным измельчением зеренной структуры материалов; гомогенизацией и перемешиванием на различных масштабных уровнях; интенсивной консолидацией порошковых материалов. Приведены инженерные соотношения для основных характеристик ВЭ. Показан прогресс в практическом применении ВЭ.

Ключевые слова: винтовая экструзия, интенсивная пластическая деформация, субмикрокристаллические материалы, простой сдвиг, измельчение зерен